# Tuning superconductivity in highly crystalline $Pb_{1-x}Bi_x$ alloy ultrathin films at atomic level

Kun Xie,[1,2,3,*] Pengju Li,[1,2,*] Liangliang Liu,[4,5,*] Runxiao Zhang,[1,2,3] Yumin Xia,[1,2,3] Haohao Shi,[1,2] Desheng Cai,[1,2,3] Yitong Gu,[1,2,3] Limin She,[6] Yeheng Song,[6] Weifeng Zhang,[6] Zhenyu Zhang,[1,3] Yu Jia,[4,5,†] and Shengyong Qin[1,2,3,‡]

[1]*International Center for Quantum Design of Functional Materials (ICQD), University of Science and Technology of China, Hefei 230026, China*

[2]*CAS Key Laboratory of Strongly-Coupled Quantum Matter Physics, Department of Physics, University of Science and Technology of China, Hefei 230026, China*

[3]*Hefei National Laboratory, University of Science and Technology of China, Hefei 230088, China*

[4]*Key Lab for Special Functional Materials of Ministry of Education, School of Materials Science and Engineering, Henan University, Kaifeng 475004, China*

[5]*Joint Center for Theoretical Physics, School of Physics and Electronics, Henan University, Kaifeng 475004, China*

[6]*Key Laboratory of Photovoltaic Materials, Henan University, Kaifeng 475004, China*

(Received 26 August 2022; revised 20 December 2022; accepted 22 February 2023; published 15 March 2023; corrected 3 April 2023)

Achieving highly crystalline superconductors with reduced dimensionality and fine-tuning their superconductivity have been daunting challenges in condensed matter physics. Here, we have successfully grown two-monolayer highly crystalline $Pb_{1-x}Bi_x(111)$ films with controllable Bi concentrations $x$ by molecular beam epitaxy and systematically studied their structural and superconducting properties by scanning tunneling microscopy. We first show that the superconducting transition temperatures of $Pb_{1-x}Bi_x$ films exhibit a domelike behavior with increasing Bi concentration $x$. Our first-principles calculations reveal that Bi doping can promote the electronic states and the electron-phonon coupling strength at lower $x$ and suppress the electron-phonon coupling strength and superconductivity with largely Bi electronic states when Bi doping increases over a critical ratio. Our findings not only demonstrate a quantum phenomenon of superconductivity in highly crystalline alloyed films but also provide a practical pathway to tune the superconductivity at the atomic level.

DOI: 10.1103/PhysRevB.107.104511

## I. INTRODUCTION

With the advancement of materials growth technology, highly crystalline superconductors in reduced dimensionality have been widely explored due to their intriguing structural and superconducting properties. In particular, tuning the superconducting properties of highly crystalline superconductors at two-dimensional limit has been the key issue in the deep understanding of the underlying mechanism of the superconductivity and has become one of the central focuses in condensed matter physics [1]. For example, the superconductivity of half-unit cell $YBa_2Cu_3O_{6+x}$ can be enhanced by hole (oxygen) doping [2], or abnormal superconductor to charge density wave phase in ultrathin $MoC_2$ crystal by Cr doping [3]. Pb is a conventional superconductor that has been widely explored for its various superconducting properties. Not only does the superconducting transition temperature ($T_c$) of Pb films oscillate with film thickness due to the quantum size effect [4,5], but Pb can also be combined with many other elements to form alloys with unique physical properties, such as the high thermal thermoelectric efficiency of PbTe [6], giant Rashba effect in PbTl films [7], and high efficiency carrier multiplication in PbSe nanocrystals [8]. In particular, by adding Bi dopant, the structural stability can be tuned, and the superconductivity of Pb films can be enhanced [9,10]. These results indicate that the superconductive pairing in bulk PbBi alloys can be altered in the quantum regime. Moreover, it has been reported that the superconductivity of Pb films persists in the two-dimensional limit [11], and the superconductivity of two-monolayer (ML) Pb films here is only one single two-dimensional subband channel, which enables us to understand the coherence and robustness of the superconducting state in quantum-mechanically confined geometries [12]. In such quantum regime, the stability and solubility of alloy ultrathin films are strongly dependent on both the substrate and the quantum size effect, which will obviously deviate from the alloy phase diagram of their bulk [13]. For example, $Pb_{1-x}Ga_x$ alloy films can be stabilized on a Si(111)-(7 × 7) substrate by quantum confinement even though Pb and Ga are immiscible in bulk form [14]. Recent theoretical work has proposed a hexagonal one-ML symmetry $Pb_3Bi/Ge(111)$ alloy system, in which not only the superconductivity was substantially enhanced by the Bi addition but also chiral topological superconductivity arises due to the type II Van Hove singularity and geometric phase [15,16]. These excellent works inspire us to explore the superconductivity of highly crystalline PbBi alloys at the two-dimensional limit by various Bi dopants and understand their underlying mechanism.

In this paper, we have successfully grown two-ML (111)-oriented highly crystalline $Pb_{1-x}Bi_x$ films on

*These authors contributed equally to this work.
†Corresponding author: jiayu@henu.edu.cn
‡Corresponding author: syqin@ustc.edu.cn

 

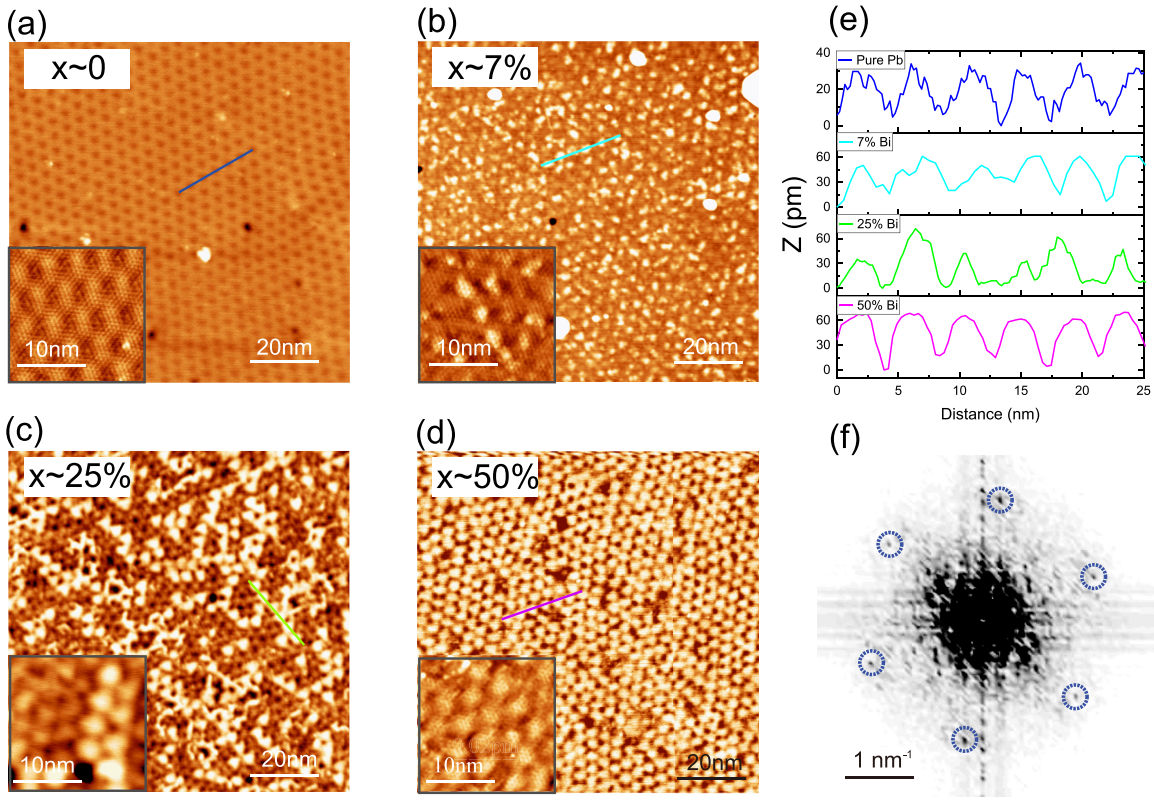


FIG. 1. STM images of two-ML $Pb_{1-x}Bi_x$ films with different Bi concentration. (a)–(d) Topography of two-ML $Pb_{1-x}Bi_x$ films with Bi concentrations of $x = 0\%$, 7%, 25%, and 50% (100 nm × 100 nm, $V = 1.5$ V, $I = 10$ pA). The insets show the atomic structures for each film (20 nm × 20 nm, $V = 0.5$ V, $I = 10$ pA). (e) The line profiles of each $Pb_{1-x}Bi_x$ film are indicated in (a)–(d). (f) The FFT image of the atomic structure of $Pb_{0.5}Bi_{0.5}$; the sixfold symmetric spots labeled with blue dashed circles correspond to the wave vector of the lattice.

Si(111) substrates with different Bi concentrations $x$ by molecular beam epitaxy (MBE) and used scanning tunneling microscopy/spectroscopy (STM/S) to systematically study their structural and superconducting properties *in situ*. We show that the surface topography of $Pb_{1-x}Bi_x$ films evolves with Bi doping, while the atomic structures remain the same, and the $T_c$ of $Pb_{1-x}Bi_x$ films increases with $x$ at first and then decreases with $x$ ($0 < x < 50\%$). First-principles calculations reveal that Bi doping can significantly promote the electronic states and the electron-phonon coupling (EPC) strength in $Pb_{1-x}Bi_x$ films at lower $x$, while as Bi doping increases, the Bi electronic states become dominant at the Fermi level ($E_F$) and in turn suppress the EPC strength and superconductivity.

## II. METHODS

All experiments were carried out in an UHV low-temperature STM system (Unisoku, USM-1500S with RHK R9 controller) with a base pressure of $\sim 1.2 \times 10^{-10}$ Torr, which was equipped with a MBE chamber for the *in situ* growth of thin films. An *n*-type Si(111) wafer with a resistivity of 0.001 cm Ω and a miscut angle of 0.1° was used as the substrate. Clean Si(111)-(7×7) substrates were prepared by a standard flash process, heated to 1150 °C with direct current and slowly cooled to room temperature several times as illustrated before [17]. Then, approximately 1.4 ML Pb (Alfa Aesar, 99.999%) was deposited on the Si(111)-(7×7) surface at 460 °C and annealed at 300 °C for 2 min to create Pb stripped-incommensurate (SIC) [18–20]. The two-ML $Pb_{1-x}Bi_x$ films were fabricated by codepositing Pb (Alfa Aesar, 99.999%) and Bi (Alfa Aesar, 99.99%) sources to the Pb SIC surface while the substrate was held at 90 K. The Pb and Bi growth rates were calibrated by depositing on a Si(111) substrate separately. By changing the source temperatures and codeposition times, two-ML $Pb_{1-x}Bi_x$ films with different ratios can be fabricated. All STM and STS measurements were taken with electrochemically etched tungsten (W) tips. The two-ML pure Pb ($x = 0$) film has two different structures ($1\times1$ and $\sqrt{3} \times \sqrt{3}$ atomic structures) with different $T_c$ values, which is consistent with a previous report [11]. From our experimental results, when the Bi concentration $x$ is less than 10%, these two structures can also be observed in $Pb_{1-x}Bi_x$ alloy films, but as the Bi concentration increases, the $1 \times 1$ structure gradually disappears, as shown in Fig. S2 in the Supplemental Material (SM) [21]. Hence, we only choose $\sqrt{3} \times \sqrt{3}$ atomic structures of two-ML $Pb_{1-x}Bi_x$ for comparison in the following discussions.

Our density functional theory (DFT) calculations were performed using the Vienna *ab initio* Simulation Package (VASP) with the projector-augmented wave method [22–24]. For the exchange-correlation energy, we employed the generalized-gradient approximation functional of Perdew-Burke-Ernzerhof [25]. The *k*-space integration was performed with a $21 \times 21 \times 1$ *k*-point grid for the $Pb_{1-x}Bi_x$ film structure optimization, and a plane-wave basis was taken with a kinetic energy cutoff of 600 eV. All atoms were allowed to

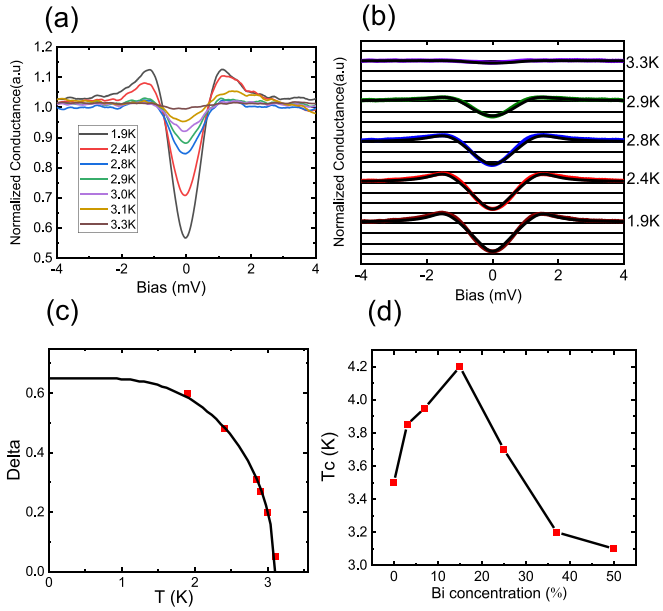


FIG. 2. Superconductivity in two-ML $Pb_{1-x}Bi_x$ films. (a) Normalized conductance spectra acquired at various temperatures for $Pb_{0.5}Bi_{0.5}$. (b) The normalized conductance spectra (nonblack colors) taken by STM were fitted using the BCS-like formula for the tunneling conductance (black). (c) The energy gaps $\Delta$ for each temperature are obtained from (b) and plotted as red squares. The transition temperature $T_c \sim 3.1$ K can be obtained by the black fitting curve using a BCS-like gap equation. (d) Two-ML $Pb_{1-x}Bi_x$ films $T_c$ varies with Bi concentration.

relax along the calculated forces until all the residual force components were less than 0.005 eV/Å, and a vacuum space of 20 Å was used to eliminate the periodic interaction in $Pb_{1-x}Bi_x$ films. The subsequent lattice dynamics and electron-phonon coupling calculations were carried out by using the QUANTUM ESPRESSO package [26] with the optimized norm-conserving Vanderbilt pseudopotentials [27] and a plane-wave cutoff of 80 Ry. Here, we used a $6 \times 6 \times 1$ $q$-point grid for the computation of phonon frequencies of $Pb_{1-x}Bi_x$ films. The Migdal-Eliashberg mechanism is employed to calculate the superconducting gap and transition temperature as implemented in the electron-phonon Wannier (EPW) code [28,29], and the interpolated $k$-point grid of $60 \times 60 \times 1$ and $q$-point grid of $30 \times 30 \times 1$ are used to calculate the superconducting properties.

## III. RESULTS AND DISCUSSIONS

### A. Experimental results

Figures 1(a)–1(d) and Fig. S2 in the SM [21] show the large-area topography images of the $Pb_{1-x}Bi_x$ films with different concentrations. Compared with pure Pb in Fig. 1(a), some bright spots appear on the $Pb_{1-x}Bi_x$ films, and these bright spots seem to distribute evenly throughout the films, as shown in Fig. 1(b). When the concentration of Bi continues to increase, the coverage of these bright spots increases [Fig. 1(c)] and they eventually form continuous moiré patterns as shown in Fig. 1(d). Figure 1(e) shows line profiles of $Pb_{1-x}Bi_x$ films with different Bi concentrations, from which all the bright spots have almost the same periodicity of approximately 4.65 nm. The high-resolution STM images [inset of Fig. 1(d)] and the fast-Fourier-transform (FFT) image in Fig. 1(f) and Fig. S3 in the SM [21] reveal the lattice constant of the $Pb_{0.5}Bi_{0.5}$ film is about 0.67 nm, in good agreement with that of $(\sqrt{3} \times \sqrt{3})$-Si (~0.667 nm). The results indicated that with Bi doping $x$ up to 50%, the $Pb_{1-x}Bi_x$ film still remains highly crystalline with a $\sqrt{3} \times \sqrt{3}$ atomic structure and lattice constant similar to those of pure Pb film [11].

To explore how the addition of Bi atoms influences the superconductivity of two-ML $Pb_{1-x}Bi_x$ alloy films, we carried out systematic STS measurements on a series of two-ML $Pb_{1-x}Bi_x$ films with different Bi concentrations $x$ ($0 < x < 50\%$). Figure 2(a) shows the typical tunneling spectra of $x = 50\%$ acquired at various temperatures. These spectra were fitted by the BCS-like density of states to obtain a temperature-dependent superconducting gap $\Delta(T)$ [see Fig. 2(b)], from which we extrapolated the $T_c \sim 3.1$ K for the $Pb_{0.5}Bi_{0.5}$ film [Fig. 2(c)].

The temperature-dependent spectra and BCS fitting of the $Pb_{1-x}Bi_x$ films with different Bi concentrations are shown in Fig. S4 in the SM [21]. Figure 2(d) summarizes the $T_c$ vs $x$ of the two-ML $Pb_{1-x}Bi_x$ films. Firstly, we can observe that $T_c$ first increases with $x$ ($0 < x < 15\%$), which is consistent with previous reports [9,10]. One possible reason is that the Bi atom has one more outmost electron than the Pb atom as conduction electrons [10]. Due to this $n$-type doping, the $Pb_{1-x}Bi_x$ alloy films have more electrons which strengthen the nesting of the Fermi surface along the (111) direction [30], leading to the enhancement of the superconductivity. More interestingly, in our measurements, the $T_c$ decreases with $x$ for higher Bi concentration ($15\% < x < 50\%$). Although the $T_c$ of up to 6 K were reported in amorphous films at high pressure [31] or Bi clusters [32], the superconductivity of bulk Bi is very weak, with a $T_c$ of only 0.5 mK [33,34]. As a result, when the doping of Bi increases, the contribution of Bi to the electronic structure and superconductivity of the $Pb_{1-x}Bi_x$ films increases and might become dominant, which eventually suppresses the film's superconductivity for higher Bi concentrations. Here we want to point out that although the $T_c$ of two-ML $Pb_{0.85}Bi_{0.15}$ film has the highest $T_c$ among all the samples we measured, taking into account the growth rate calibrations and other measurement errors, it might be difficult to precisely determine the Bi ratio of the two-ML $Pb_{1-x}Bi_x$ films with the maximum value of $T_c$. However, our experimental results unambiguously demonstrated that the $T_c$ of $Pb_{1-x}Bi_x$ films show a domelike behavior with increasing Bi concentrations. Moreover, in the two-ML $Pb_{1-x}Bi_x$ alloyed films, the BCS ratios $2\Delta(0)/k_BT_c$ are calculated to range from 4.0 to 4.8, which indicates that the $Pb_{1-x}Bi_x$ alloy films are strong-coupled superconductors. The observed high coupling strength implies the presence of strong coupling between the electrons and low-lying phonons, which is consistent with earlier work using electron tunneling spectroscopy [35–37].

It has been reported that the existence of moiré patterns in two-dimensional material superlattices or heterostructures will greatly impact their electronic structures [38–42]. In the two-ML $Pb_{1-x}Bi_x$ films here, the topography of the moiré patterns also depends on the Bi concentrations. Here we measured $dI/dV$ spectra in both bright spots and dark

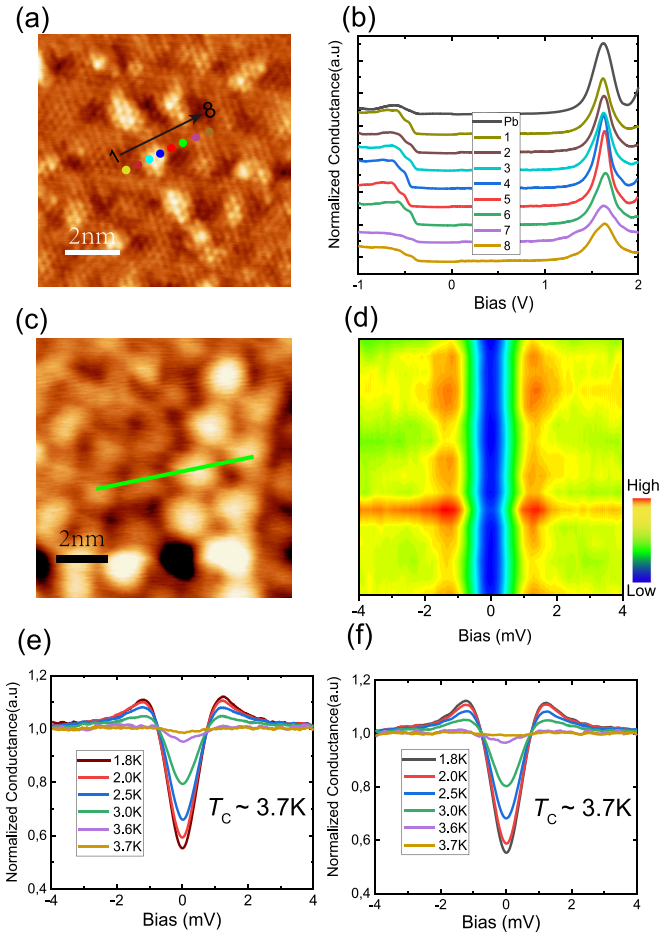


FIG. 3. (a) Atomic structure of two-ML $Pb_{0.93}Bi_{0.07}$ film (10 nm × 10 nm, $V = 5$ mV, $I = 10$ pA). (b) $dI/dV$ spectra of $Pb_{0.93}Bi_{0.07}$ film taken at the dotted line (labeled as 1 to 8) in (a); the black $dI/dV$ curve is on pure Pb film for comparison. (c) STM image of $Pb_{0.75}Bi_{0.25}$ films (10 nm × 10 nm, $V = 5$ mV, $I = 10$ pA). (d) Scanning tunneling spectroscopy measurements across different spots along the green line indicated in (a) at 1.8 K. The superconducting spectra appear homogeneous across the bright spot. (e),(f) The temperature-dependent spectra in bright spots and dark areas, respectively. There is no obvious difference in the $dI/dV$ spectra and the extrapolated superconducting $T_c$.

areas. Figures 3(a) and 3(b) show the STM image of two-ML $Pb_{0.93}Bi_{0.7}$ film and the corresponding $dI/dV$ spectra across a bright spot. It can be seen that the peak positions of the quantum well states (QWS) of the $Pb_{1-x}Bi_x$ alloy film are similar to those of pure Pb film [11], suggesting the QWS of the $Pb_{1-x}Bi_x$ alloy film is mainly dominated by Pb. Moreover, we also carried out superconductivity spectra measurements across the bright spots and dark areas on the moiré patterns of the two-ML $Pb_{0.75}Bi_{0.25}$ films [see Figs. 3(c) and 3(d)], and Figs. 3(e) and 3(f) which show all temperature-dependent spectra on both bright spots and dark areas, indicating that the superconductivity is homogeneous across the moiré patterns of the $Pb_{1-x}Bi_x$ films. We attribute this homogeneity in superconductivity to the fact that Pb has a large coherence length of approximately 90 nm [43], which is much larger than the moiré pattern size.

### B. Calculational results

In addition to the *n*-type doping effect discussed above, how the Bi atoms affect the electronic states and, more importantly, the EPC of the $Pb_{1-x}Bi_x$ films and the underlying mechanism still need further exploration. Here, we perform first-principles calculations of the electronic and phononic properties of different two-ML $Pb_{1-x}Bi_x$ films from which large EPC is derived [44], and make comparative discussions of Bi concentrations of $x = 25\%$ and 50% with pure Pb film. To this end, a $2 \times 2$ Pb supercell on $(\sqrt{3} \times \sqrt{3})$-Si(111) substrate were constructed to simulate the $Pb_{0.75}Bi_{0.25}$ and $Pb_{0.5}Bi_{0.5}$ crystalline alloy films where two or four Pb atoms are replaced by Bi atoms, respectively [see Fig. 4(a) and Fig. S5 in the SM [21]]. The estimated $T_c$ of $Pb_{1-x}Bi_x$ alloy films by solving the Eliashberg equations [45] are shown in Fig. 5(b), together with the case of pure Pb film for comparison. In this estimation, different Coulomb pseudopotential parameters $\mu^\star$ are used for different Bi concentrations in the $Pb_{1-x}Bi_x$ films [36]. The $T_c$ of the pure Pb film is ~5.0 K, which is comparable to the experimental value of $T_c \sim 3.7$ K. When the concentration of Bi doping is 25%, $T_c$ is increased to ~6.6 K, and is higher than that of the pure Pb film. By increasing the concentration of Bi doping up to 50%, the $T_c$ becomes ~4.7 K. The DFT calculations are qualitatively consistent with our experimental observation that with Bi doping, the $T_c$ of $Pb_{1-x}Bi_x$ films starts to increase while the $T_c$ turns to decrease in Bi overdoped $Pb_{1-x}Bi_x$ film.

To reveal the underlying mechanism of the domelike behavior of $T_c$ as the Bi concentration increases and gain a better understanding of the enhancement of the superconducting properties of Bi in Pb films, we calculated the electronic structures of pure Pb, $Pb_{0.75}Bi_{0.25}$, and $Pb_{0.5}Bi_{0.5}$ films. The calculated band structures and partial electronic densities of states are displayed in Figs. 4(a) and 5(b). Compared with the pure Pb film, we note that with *n*-type doping of Bi into the Pb film, more bands are turned to be across the $E_F$, and the corresponding electronic occupations of Pb atoms in $Pb_{1-x}Bi_x$ alloy films become considerably large, associated with an emergent peak near $E_F$, which could be beneficial for the superconductivity of $Pb_{1-x}Bi_x$ films. The quantitative evaluation of EPC strength λ for $Pb_{1-x}Bi_x$ and pure Pb films is shown in Fig. 5(c). As expected, the obtained total λ of the $Pb_{0.75}Bi_{0.25}$ film is 1.15, which is larger than the $\lambda = 0.79$ of the pure Pb film due to the low-frequency vibration modes (2–5 meV) of Pb and Bi atoms in the $Pb_{0.75}Bi_{0.25}$ film, leading to the enhancement of coupling with electronic states on the Fermi surface (FS). We also note that Bi electronic states in the $Pb_{1-x}Bi_x$ film become the dominant component near $E_F$ with more concentrations of Bi up to 50%, and in turn, the relative proportion of Pb electronic states on the FS decreases. This means that the EPC strength in the $Pb_{0.5}Bi_{0.5}$ film weakens because of very weak vibration interactions between Bi atoms [33]. This can be manifested by the spectral function $\alpha^2F(\omega)$, which peaks at a low frequency of 2–5 meV [see the middle panel of Fig. 5(c)]. Therefore, the total λ of the $Pb_{0.5}Bi_{0.5}$ film is 0.95, and the estimated $T_c$ is ~4.7 K, smaller than both pure Pb and $Pb_{0.75}Bi_{0.25}$ films.

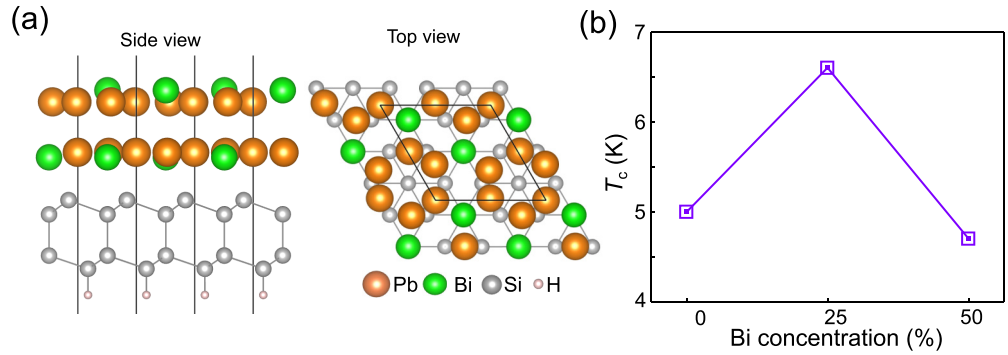


FIG. 4. First-principles calculations of two-ML $Pb_{1-x}Bi_x$ alloy films. (a) Structural model of the $Pb_{0.75}Bi_{0.25}$ film on the $(\sqrt{3} \times \sqrt{3})$-Si(111) surface. (b) The estimated $T_c$ of two-ML pure Pb (0%), $Pb_{0.75}Bi_{0.25}$ (25% Bi), and $Pb_0.5Bi_0.5$ (50% Bi) films.

## IV. CONCLUSION

In conclusion, by combining STM measurements and first-principles calculations, we have systematically studied the atomic structures and superconductivity of two-ML highly crystalline $Pb_{1-x}Bi_x$ $(0 < x < 50\%)$ films by controlling the Bi concentrations. Our results show that Bi doping can significantly promote the Pb electronic states and the EPC strength in $Pb_{1-x}Bi_x$ films that enhance the $T_c$ at lower $x$, while as the concentration of Bi doping increases, the Bi electronic states become dominant components at the $E_F$ and in turn suppress the EPC strength and superconductivity. Our results offer an angle to tune the superconductivity at the atomic levels and uncover the underlying mechanism of highly crystalline superconductors at two-dimensional limit. Furthermore, the present study might provide a candidate material to realize intrinsic chiral topological superconductivity.

## ACKNOWLEDGMENTS

This work was supported by the National Key Basic Research Program of China (Grant No. 2017YFA0205004), the National Natural Science Foundation of China (Grants No. 92165201, No. 11634011, No. 11474261, No. 12104129,

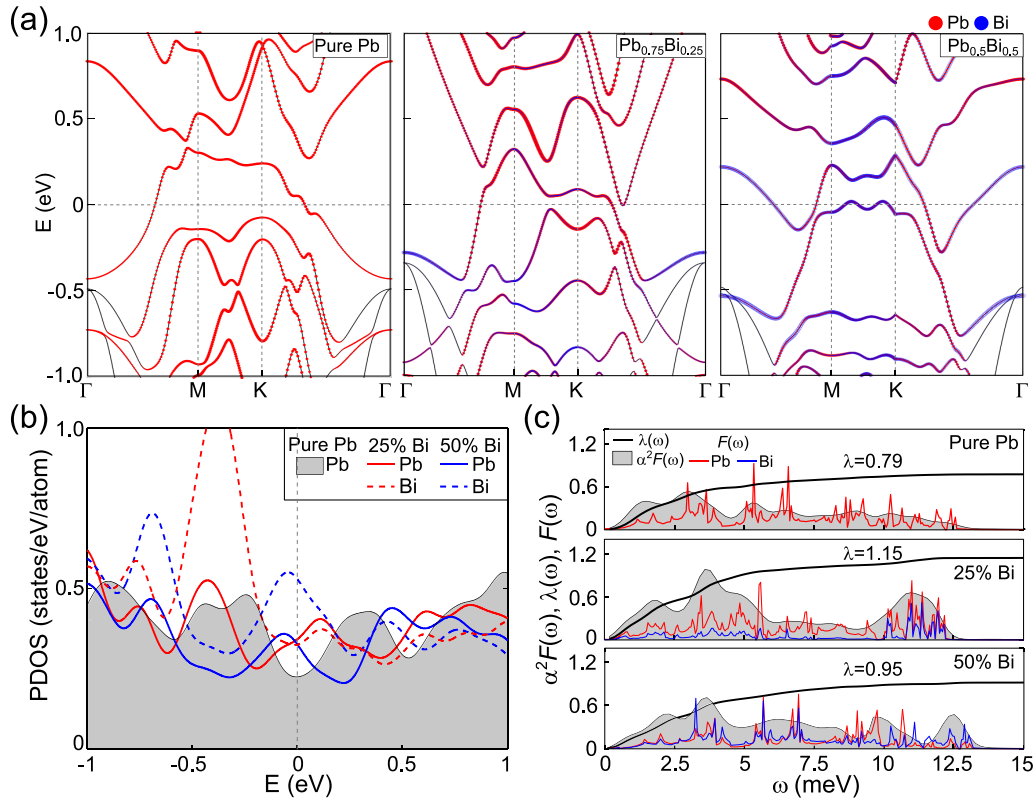


FIG. 5. (a) The band structures of pure Pb, $Pb_{0.75}Bi_{0.25}$, and $Pb_0.5Bi_0.5$ films with the projection onto the atoms Pb and Bi. (b) The partial density of states per atom (PDOS) of pure Pb, $Pb_{0.75}Bi_{0.25}$, and $Pb_{0.5}Bi_{0.5}$ films for comparison. (c) The atom-projected phonon density of states $F(\omega)$, Eliashberg spectral function $\alpha^2F(\omega)$, and integrated EPC constant $\lambda(\omega)$ for pure Pb, $Pb_{0.75}Bi_{0.25}$, and $Pb_{0.5}Bi_{0.5}$ films.

and No. 12074099), Innovation Program for Quantum Science and Technology (2021ZD0302800), the Anhui Initiative in Quantum Information Technologies (Grant No. AHY170000), and the Fundamental Research Funds for the Central Universities (Grants No. WK3510000006 and No. WK3430000003).

[1] Y. Saito, T. Nojima, and Y. Iwasa, Highly crystalline 2D superconductors, Nat. Rev. Mater. **2**, 16094 (2016).

[2] B. Ramshaw, S. Sebastian, R. McDonald, J. Day, B. Tan, Z. Zhu, J. Betts, R. Liang, D. Bonn, W. Hardy *et al.*, Quasiparticle mass enhancement approaching optimal doping in a high-$T_c$ superconductor, Science **348**, 317 (2015).

[3] S. Li, Z. Zhang, C. Xu, Z. Liu, X. Chen, Q. Bian, H. Gedeon, Z. Shao, L. Liu, Z. Liu *et al.*, Magnetic doping induced superconductivity-to-incommensurate density waves transition in a 2D ultrathin Cr-doped $Mo_2C$ crystal, ACS Nano **15**, 14938 (2021).

[4] Y. Guo, Y.-F. Zhang, X.-Y. Bao, T.-Z. Han, Z. Tang, L.-X. Zhang, W.-G. Zhu, E. Wang, Q. Niu, Z. Qiu *et al.*, Superconductivity modulated by quantum size effects, Science **306**, 1915 (2004).

[5] D. Eom, S. Qin, M.-Y. Chou, and C. K. Shih, Persistent Superconductivity in Ultrathin Pb Films: A Scanning Tunneling Spectroscopy Study, Phys. Rev. Lett. **96**, 027005 (2006).

[6] Y. Pei, A. LaLonde, S. Iwanaga, and G. J. Snyder, High thermoelectric figure of merit in heavy hole dominated PbTe, Energy Environ. Sci. **4**, 2085 (2011).

[7] A. Matetskiy, S. Ichinokura, L. V. Bondarenko, A. Y. Tupchaya, D. V. Gruznev, A. V. Zotov, A. A. Saranin, R. Hobara, A. Takayama, and S. Hasegawa, Two-Dimensional Superconductor with a Giant Rashba Effect: One-Atom-Layer Tl-Pb Compound on Si(111), Phys. Rev. Lett. **115**, 147003 (2015).

[8] R. D. Schaller and V. I. Klimov, High Efficiency Carrier Multiplication in PbSe Nanocrystals: Implications for Solar Energy Conversion, Phys. Rev. Lett. **92**, 186601 (2004).

[9] M. M. Ozer, Y. Jia, Z. Zhang, J. R. Thompson, and H. H. Weitering, Tuning the quantum stability and superconductivity of ultrathin metal alloys, Science **316**, 1594 (2007).

[10] Y. Jia, S. Y. Wang, W. G. Chen, Q. Sun, H. H. Weitering, and Z. Zhang, First-principles study of quantum size effects in ultrathin Pb-Bi metal alloy films, Phys. Rev. B **81**, 245425 (2010).

[11] S. Qin, J. Kim, Q. Niu, and C.-K. Shih, Superconductivity at the two-dimensional limit, Science **324**, 1314 (2009).

[12] H. H. Weitering, The world's thinnest superconductor, Chem. Phys. Chem. **10**, 3183 (2009).

[13] F. Besenbacher, I. Chorkendorff, B. Clausen, B. Hammer, A. Molenbroek, J. K. Nørskov, and I. Stensgaard, Design of a surface alloy catalyst for steam reforming, Science **279**, 1913 (1998).

[14] E. J. Moon, M. M. Özer, Y. Jia, G. Duscher, J. R. Thompson, Z. Y. Zhang, and H. H. Weitering, Quantum stability and superconducting properties of ultrathin alloy films made from bulk immiscible elements: Pb and Ga, Phys. Rev. B **84**, 125415 (2011).

[15] W. Qin, L. Li, and Z. Zhang, Chiral topological superconductivity arising from the interplay of geometric phase and electron correlation, Nat. Phys. **15**, 796 (2019).

[16] L. Li, S. Ren, W. Qin, S. Zhang, X. Wan, Y. Jia, P. Cui, and Z. Zhang, Emergence of Van Hove singularity and topological states in $Pb_3Bi$/Ge(111) Rashba systems, Phys. Rev. B **102**, 035150 (2020).

[17] F. Cai, P. Li, K. Xie, R. Tang, and S. Qin, Superconductivity of Pb films studied with superconducting Pb tips, Sci. China Phys. Mech. Astron. **62**, 17421 (2019).

[18] E. Ganz, H. Ing-Shouh, X. Fulin, S. K. Theiss, and J. Golovchenko, Growth and morphology of Pb on Si(111), Surf. Sci. **257**, 259 (1991).

[19] E. Ganz, F. Xiong, I. S. Hwang, and J. Golovchenko, Submonolayer phases of Pb on Si(111), Phys. Rev. B **43**, 7316 (1991).

[20] L. Seehofer, G. Falkenberg, D. Daboul, and R. L. Johnson, Structural study of the close-packed two-dimensional phases of Pb on Ge(111) and Si(111), Phys. Rev. B **51**, 13503 (1995).

[21] See Supplemental Material at http://link.aps.org/supplemental/10.1103/PhysRevB.107.104511 for details of more STM images and STS spectra of two-ML PbBi films, calculational models, and the calculated superconducting gap of each two-ML PbBi film.

[22] G. Kresse and J. Hafner, *Ab initio* molecular dynamics for open-shell transition metals, Phys. Rev. B **48**, 13115 (1993).

[23] P. E. Blöchl, Projector augmented-wave method, Phys. Rev. B **50**, 17953 (1994).

[24] G. Kresse and J. Furthmüller, Efficiency of ab-initio total energy calculations for metals and semiconductors using a plane-wave basis set, Comput. Mater. Sci. **6**, 15 (1996).

[25] J. P. Perdew, K. Burke, and M. Ernzerhof, Generalized Gradient Approximation Made Simple, Phys. Rev. Lett. **77**, 3865 (1996).

[26] P. Giannozzi, S. Baroni, N. Bonini, M. Calandra, R. Car, C. Cavazzoni, D. Ceresoli, G. L. Chiarotti, M. Cococcioni, I. Dabo *et al.*, QUANTUM ESPRESSO: a modular and open-source software project for quantum simulations of materials, J. Phys.: Condens. Matter **21**, 395502 (2009).

[27] M. J. van Setten, M. Giantomassi, E. Bousquet, M. J. Verstraete, D. R. Hamann, X. Gonze, and G.-M. Rignanese, The PseudoDojo: Training and grading a 85 element optimized norm-conserving pseudopotential table, Comput. Phys. Commun. **226**, 39 (2018).

[28] F. Giustino, M. L. Cohen, and S. G. Louie, Electron-phonon interaction using Wannier functions, Phys. Rev. B **76**, 165108 (2007).

[29] S. Poncé, E. R. Margine, C. Verdi, and F. Giustino, EPW: Electron–phonon coupling, transport and superconducting properties using maximally localized Wannier functions, Comput. Phys. Commun. **209**, 116 (2016).

[30] Y. Jia, B. Wu, C. Li, T. L. Einstein, H. H. Weitering, and Z. Zhang, Strong Quantum Size Effects in Pb(111) Thin Films Mediated by Anomalous Friedel Oscillations, Phys. Rev. Lett. **105**, 066101 (2010).

[31] T. Hamada, K. Yamakawa, and F. Fujita, Superconductivity of vacuum-deposited bismuth films, J. Phys. F **11**, 657 (1981).

[32] B. Weitzel and H. Micklitz, Superconductivity in Granular Systems Built from Well-Defined Rhombohedral Bi-Clusters: Evidence for Bi-Surface Superconductivity, Phys. Rev. Lett. **66**, 385 (1991).

[33] O. Prakash, A. Kumar, A. Thamizhavel, and S. Ramakrishnan, Evidence for bulk superconductivity in pure bismuth single crystals at ambient pressure, Science **355**, 52 (2017).

[34] Z. Mata-Pinzón, A. A. Valladares, R. M. Valladares, and A. Valladares, Superconductivity in bismuth. A new look at an old problem, PLoS One **11**, e0147645 (2016).

[35] J. Adler and T. Chen, Strong coupling superconductivity of $Pb_{0.7}Bi_{0.3}$ alloys, Solid State Commun. **9**, 1961 (1971).

[36] P. B. Allen and R. Dynes, Transition temperature of strong-coupled superconductors reanalyzed, Phys. Rev. B **12**, 905 (1975).

[37] P. Butcher and L. Yu, *Superconductivity: From Basic Physics to the Latest Developments—Lecture Notes of the Ictp Spring College in Condensed Matter on Superconductivity* (World Scientific, Singapore, 1995).

[38] Z. Y. Rong and P. Kuiper, Electronic effects in scanning tunneling microscopy: Moiré pattern on a graphite surface, Phys. Rev. B **48**, 17427 (1993).

[39] K. Kobayashi and J. Yamauchi, Electronic structure and scanning-tunneling-microscopy image of molybdenum dichalcogenide surfaces, Phys. Rev. B **51**, 17085 (1995).

[40] J. Kang, J. Li, S.-S. Li, J.-B. Xia, and L.-W. Wang, Electronic structural Moiré pattern effects on $MoS_2/MoSe_2$ 2D heterostructures, Nano Lett. **13**, 5485 (2013).

[41] S. Carr, S. Fang, and E. Kaxiras, Electronic-structure methods for twisted Moiré layers, Nat. Rev. Mater. **5**, 748 (2020).

[42] H. Shi, Z. Zhan, Z. Qi, K. Huang, E. v. Veen, J. Á. Silva-Guillén, R. Zhang, P. Li, K. Xie, H. Ji *et al.*, Large-area, periodic, and tunable intrinsic pseudo-magnetic fields in low-angle twisted bilayer graphene, Nat. Commun. **11**, 371 (2020).

[43] R. F. Gasparovic and W. McLean, Superconducting penetration depth of lead, Phys. Rev. B **2**, 2519 (1970).

[44] I. Y. Sklyadneva, R. Heid, K.-P. Bohnen, P. M. Echenique, and E. V. Chulkov, Electron-phonon coupling and superconductivity in the (4/3)-monolayer of Pb on Si(111): Role of spin-orbit interaction, Phys. Rev. B **97**, 195409 (2018).

[45] G. Eliashberg, Interactions between electrons and lattice vibrations in a superconductor, Sov. Phy.-JETP **11**, 696 (1960).

*Correction:* The name of the 12th author contained an error and has been fixed.